

Towards a shielding design for the momentum cleaning insertion of the LHC

I. L. Azhgirey*, I. S. Baishev*, M. Brugger, J. B. Jeanneret,
I. A. Kourotchkine* and G. R. Stevenson

Keywords: optics, collimation, cascade, shielding, dose, fluence

Summary

A model of the momentum cleaning insertion was set up for use with the cascade simulation program MARS. This has been used to determine parameters for shielding design. Two possible variants have been considered in detail. The criteria of an optimised shield for the momentum cleaning insertion of the LHC are discussed.

1 Introduction

One goal of an effective shielding design in the momentum cleaning system is to prevent quenches in the super-conducting magnets induced by the hadronic and electromagnetic showers initiated by particle losses. Another is to limit damage to equipment installed outside the shielding and to reduce the radiation exposure of maintenance personnel to acceptable values. This is achieved in three stages [1]:

- Identification of the source terms.
- Specification of the design levels for the radiological constraints.
- Design of the actual shield on an optimum cost-effective basis with readily available construction materials.

The identification of the sources in the momentum cleaning insertion is given in [4]. It is assumed that 1.0×10^{16} protons per year will be lost on the collimator jaws in the

*Institute for High Energy Physics, Protvino, Russia.

Member of the Russian collaboration to the LHC Project.

This is an internal CERN publication and does not necessarily reflect the views of the LHC project management.

nominal conditions of operation [5]. These primary losses in the momentum cleaning will be distributed among 7 collimators for each of the two rings.

The specification of the design levels for the radiological constraints due to induced radioactivity is still being developed. It is unreasonable in a design phase to expect that all persons performing maintenance work should receive the CERN reference dose of 15 mSv in one year. It is impossible to plan maintenance operations from this far ahead of time with an accuracy sufficient to avoid exceeding this reference value. Estimates of the dose rates from induced radioactivity can also be inaccurate. It is thus reasonable to plan maintenance operations with a Design Limit for the Annual Dose of 5 mSv. In order to meet this goal, the following guidelines must be used. In Chapter VI, section 1.4 of the INB Rapport Préliminaire [6] it was written:

... but for the design and construction of accelerator components which will become active, the following dose rate reference values have proved to be very useful:

1. **100 μ Sv/h:** In regions where the dose rates are below this value, persons may work on the radioactive components without special precautions. Above this value all work must be planned, especially with respect to its duration.
2. **2 mSv/h:** Above this value the intervention time in the zone must be severely limited and all work must be supervised by RP Group. Workers from firms outside CERN who only have a temporary contract with the firm are not allowed to work in these zones. When dose rates exceed this value, remote handling of the components concerned should be seriously envisaged.
3. **20 mSv/h:** In regions where dose rates are above this value, no work is allowed since dose limits would be too easily exceeded. Remote handling of objects is essential.

Apart from the constraints mentioned above, one must consider radiation hardness, thermal expansion, stresses and maximum power deposition density. The dose to the coils of the warm magnets in the cleaning insertions must not exceed 50 MGy, and the steady quench limits of the superconducting coils are close to 5 mW cm⁻³ [7]. In order to reduce doses to the magnets coils a design of shielding screens and passive collimators has already been proposed in [4, 8]

This report contains a discussion of an optimised shielding design and of scenarios of shielding installation in the LHC tunnel. The aim is to optimise the volume and the cost of the shielding while preserving its efficiency. Specific radiological aspects of this problems will be presented in a separate report.

2 The momentum cleaning insertion in IR3

A discussion of the optics used for a momentum cleaning insertion can be found in [2][3]. The cleaning section proper consists of conventional magnets to avoid quenches and high

heat loads to cryogenics. One-half of the cleaning insertion is illustrated schematically in Figure 1. The outer quadrupoles are super-conducting, Q6L (upstream) and Q6R (far downstream) of the collimators. A pair of warm bending magnets, D4L and D3L, increases the beam separation locally from 194 to 224 mm while another pair D3R and D4R restores the nominal separation. The machine section considered here starts at the entrance to the quadrupole Q6L and finishes at the end of the quadrupole Q6R.

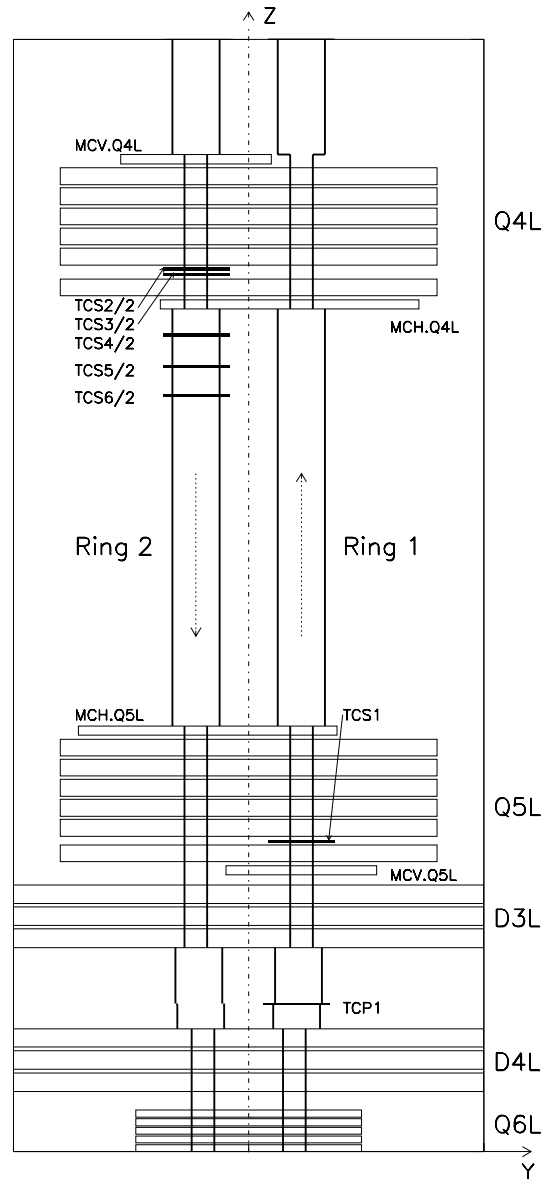


Figure 1: Layout of one half of the cleaning section.

3 The Shielding Design

The shielding for the momentum cleaning insertion starts downstream of the dipole D4L and ends with the passive collimator just upstream of D4R. This passive collimator is used to prevent quenches in the super-conducting quadrupoles Q6 and is described in [8]. Its cross-section is shown in Figure 2. It will be included in future versions of the optics sequence as a separate element.

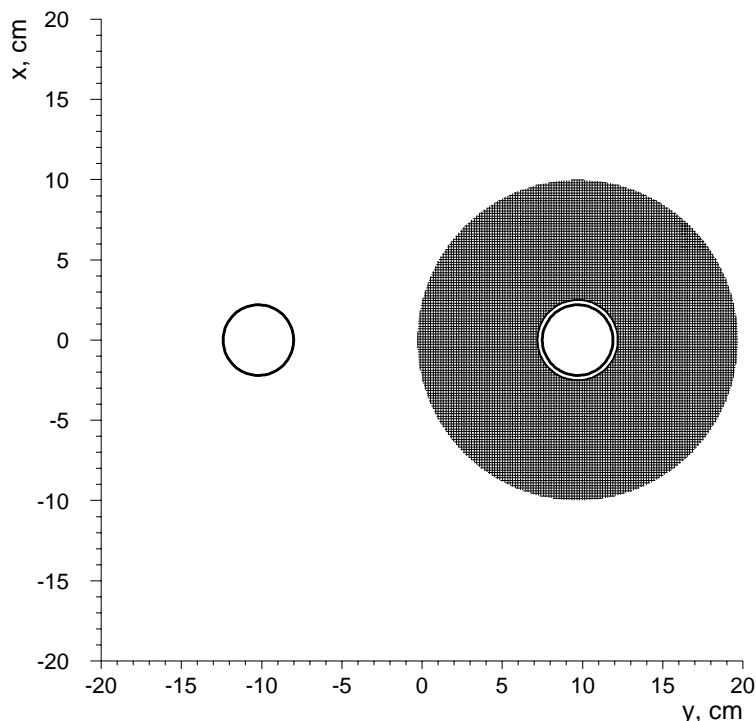


Figure 2: Cross-section of the passive collimator for Q6.

The screens shielding the coils of the warm dipoles and corrector magnets are included in the current shielding design of the momentum cleaning insertion. The transverse cross-sections of the regular shielding for the short and long drift sections are shown in Figures 3 and 4. The outer dimensions of the shielding are defined by the passage-way and transportation needs; the inner dimensions are defined by the outer size of the beam pipes and an acceptable gap for their installation.

The transverse cross-sections of the shielding around the collimator tank with its motor for the primary collimator and the secondary collimator are illustrated in Figures 5 and 6, respectively. Around a collimator tank the outer dimensions of the shielding are defined by the outer dimensions of the warm quadrupole. The inner dimensions are defined by the circle which contains the motor blocks; these can be located at any azimuthal angle with respect to the beam. It should be noted that an effective shield must be placed as close as possible to the beam pipes or collimators.

One half of the momentum cleaning section with its shielding is shown schematically in Figure 7, and a full list of the shielding elements together with their longitudinal positions and lateral dimensions is given in Table 1. The iron shielding covers not only the long drift section but also some sections inside the warm separation quadrupole modules.

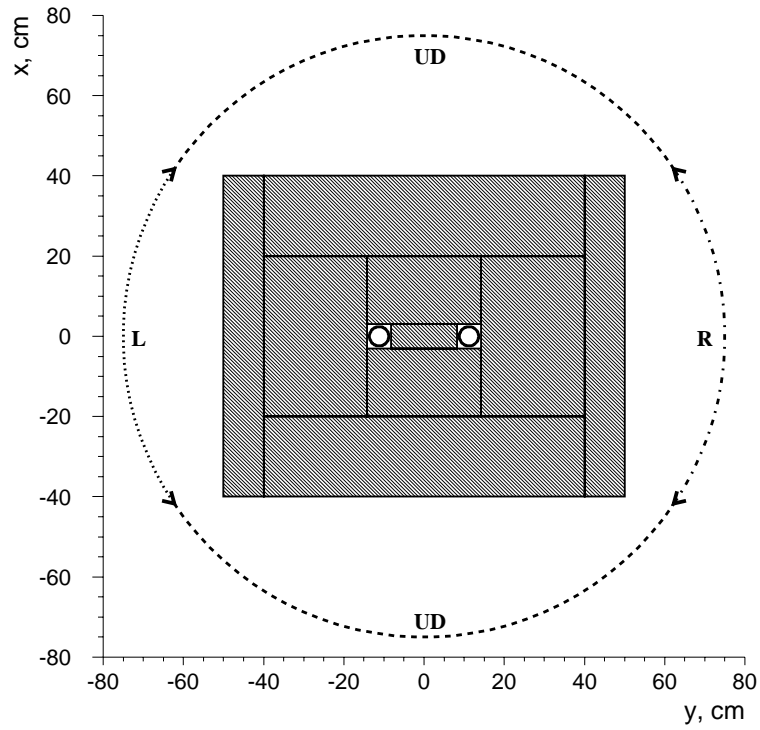


Figure 3: Cross-section of the shielding around the beam pipe of 48 mm diameter.

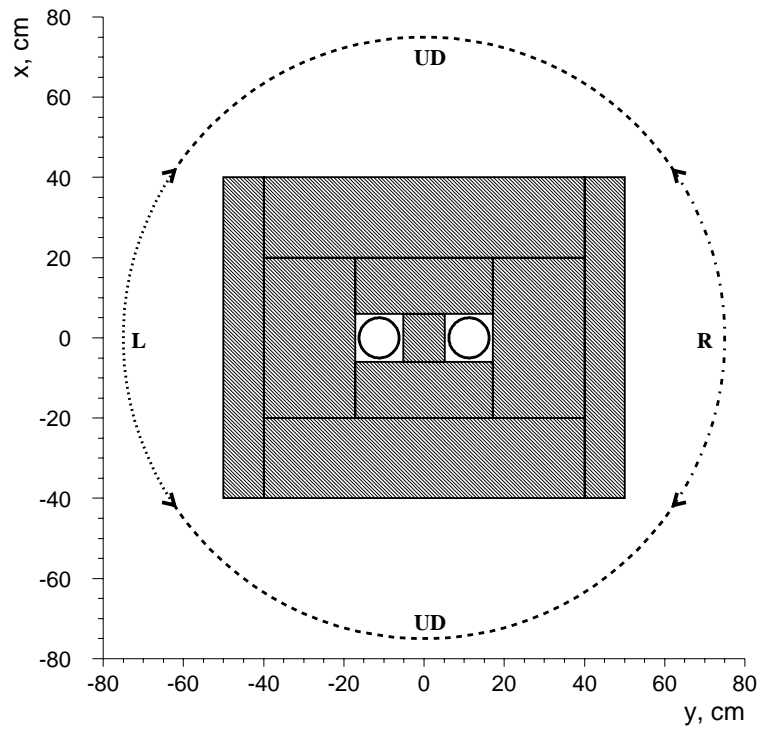


Figure 4: Cross-section of the shielding around the beam pipe of 105 mm diameter.

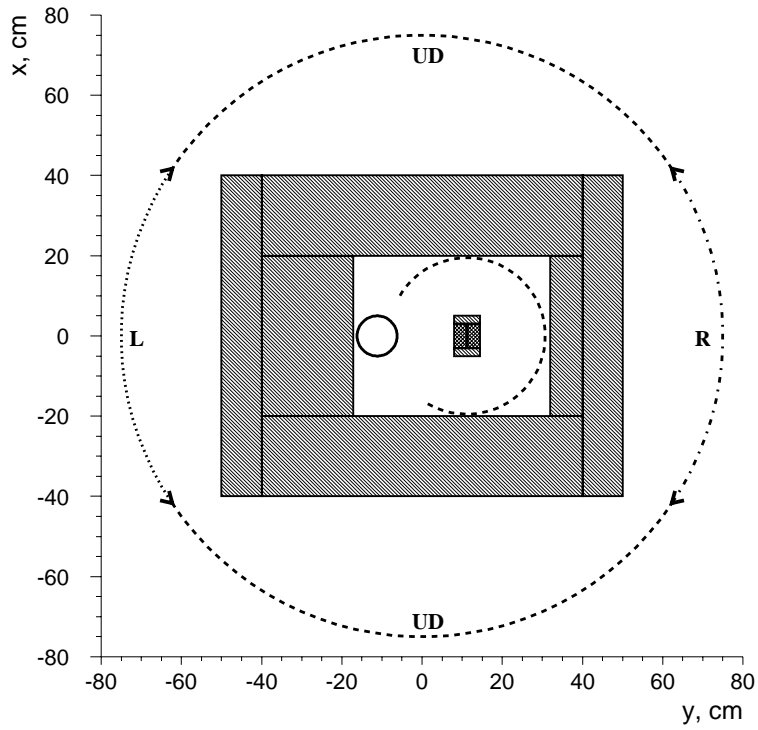


Figure 5: Cross-section of the shielding around the beam pipe and a primary collimator tank.

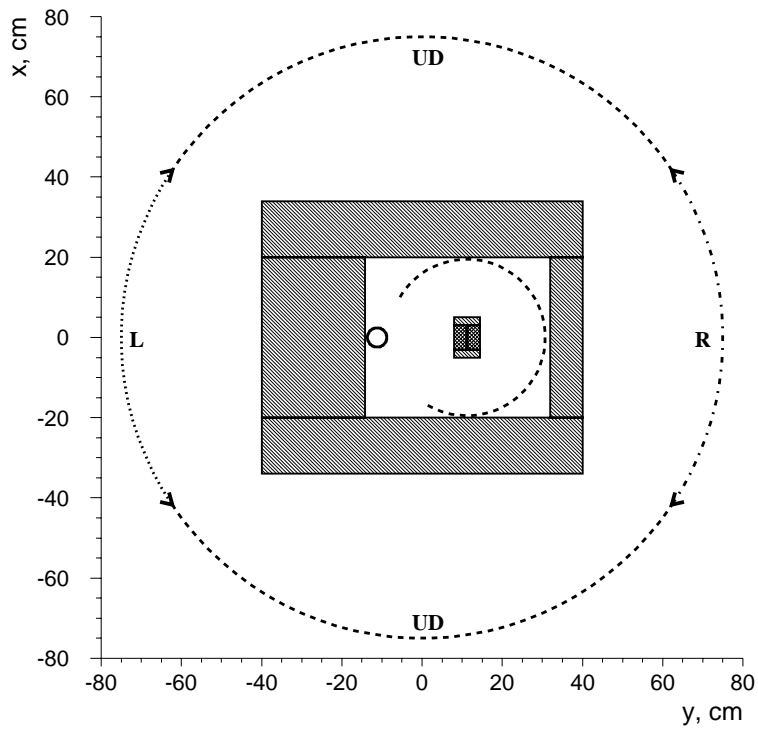


Figure 6: Cross-section of the shielding around the beam pipe and a secondary collimator tank located between the MQW modules.

The total length of this shielding is about 220 m. Such a shield will require approximately 1400 tons of iron for its realization. In addition, about 240 tons of concrete are required for the shielding supports.

4 Results and discussion

For the simulation of the hadronic and electromagnetic cascades in the momentum cleaning the MARS code was used [9]. The source terms were obtained with the K2 [10] code which provides a multi-turn impact map of the protons on the collimators. The transport of hadrons was followed down to 10 MeV for the fluence and energy deposition calculations. For estimating induced radioactivity, an energy cutoff of 50 MeV was used.

4.1 Hadron leakage

The local hadron fluence and the average hadron energy are indicators of the magnitude of induced radioactivity in air, ground-water, rock and cooling water. The longitudinally averaged values of the leakage of hadrons through the cylindrical scoring shell indicated in Figures 3 to 6 are presented in Table 2 for the collimation systems in the insertions IR3 and IR7 (taken from previous studies [11, 12, 13]. The total energy, total hadron current and average energy of hadrons passing through the scoring shell are also given. Data are given for the cases of no shielding and for the full shielding described previously. For completeness the case of a shield that will be discussed later in this paper (the “reduced” shield) is also given for the momentum scrapers. The data from Table 2 show that the efficiency of the shielding design is almost the same for the betatron and momentum cleaning. It is interesting to note that both the hadron leakage current and mean energy are a factor two lower with the shielding. This is very similar to the reduction obtained in the 1992 study of the scraper systems [14] for inelastic hadronic interactions (stars) in the rock surrounding the tunnel.

The longitudinal distribution of hadron fluence in a cylindrical scoring shell of radius 70 cm and situated symmetrically around the beam pipes is shown in Figure 8 with and without shielding at top energy. All results presented in these figures are normalized to 1.0×10^{16} protons interacting inelastically in each of the two scraper channels (beams 1 and 2).

As can be seen from Figure 8 the main peaks of the distribution are concentrated around collimators TCS1-TCS3 since most of the secondary particles coming from the primary collimator are intercepted by the jaws of the secondary collimators. Smaller peaks are located around shielding screens which serve to decrease the radiation loads to the magnet coils. However it is interesting to note that the full shielding is most efficient in regions where the leakage fluence is not the most important, *i.e.* in the long drift regions between the quadrupoles Q4 and Q5.

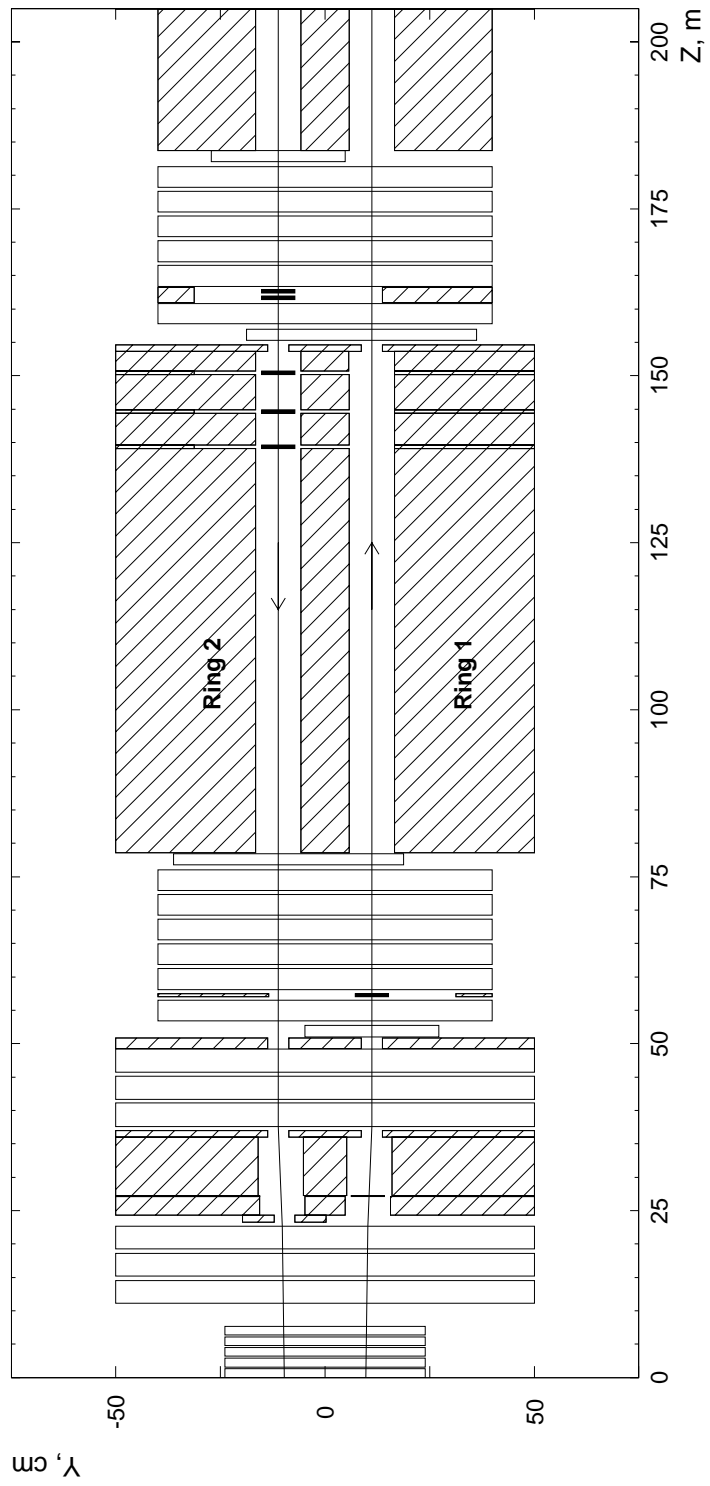


Figure 7: Longitudinal section through one half of the cleaning section for the full shielding configuration.

Table 1: Sequence and dimensions of shielding elements in the momentum cleaning for optics version 6.2.

Name	Entrance [m]	Length [m]	Outer dimensions		Inner dimensions	
			H(or R),cm	V, cm	h(or r), cm	v, cm
Passive collimator for Q6L	23.298	1.000	10.0		2.5	
Shield	24.298	2.792	50.0	40.0	16.2	6.0
Sh.box for TCP1	27.090	0.200	50.0	40.0	-15.6 – 30.3	20.0
Shield	27.290	8.691	50.0	40.0	16.6	6.0
Sh.screen for D3L	35.981	1.000	50.0	40.0	13.7	2.5
Sh.screen for MCVQ5L	49.844	0.500	50.0	40.0	13.7	2.5
Shield	56.674	0.331	40.0	35.0	14.2	3.0
Sh.box for TCS1	57.005	0.500	40.0	35.0	-13.7 – 31.3	20.0
Shield	57.505	0.469	40.0	35.0	14.2	3.0
Shield	78.604	60.526	50.0	40.0	17.2	6.0
Sh.box for TCS6/2	139.130	0.500	50.0	40.0	-31.3 – 16.6	20.0
Shield	139.630	4.740	50.0	40.0	17.2	6.0
Sh.box for TCS5/2	144.370	0.500	50.0	40.0	-31.3 – 16.6	20.0
Shield	144.870	5.320	50.0	40.0	17.2	6.0
Sh.box for TCS4/2	150.190	0.500	50.0	40.0	-31.3 – 16.6	20.0
Shield	150.690	2.935	50.0	40.0	17.2	6.0
Sh.screen for MCHQ4L	153.625	1.000	50.0	40.0	13.7	2.5
Shield	160.955	0.471	40.0	35.0	14.2	3.0
Sh.box for TCS3/2	161.426	0.500	40.0	35.0	-31.3 – 13.7	20.0
Shield	161.926	0.50	40.0	35.0	14.2	3.0
Sh.box for TCS2/2	162.426	0.500	40.0	35.0	-31.3 – 13.7	20.0
Shield	162.926	0.329	40.0	35.0	14.2	3.0
Shield	183.885	41.510	40.0	35.0	17.2	6.0
Shield	246.025	0.329	40.0	35.0	14.2	3.0
Sh.box for TCS2	246.354	0.500	40.0	35.0	-13.7 – 31.3	20.0
Shield	246.854	0.500	40.0	35.0	14.2	3.0
Sh.box for TCS3	247.354	0.500	40.0	35.0	-13.7 – 31.3	20.0
Shield	247.854	0.471	40.0	35.0	14.2	3.0
Sh.screen for MCHQ4R	254.655	1.000	50.0	40.0	13.7	2.5
Shield	255.655	2.935	50.0	40.0	17.2	6.0
Sh.box for TCS4	258.590	0.500	50.0	40.0	-16.6 – 31.3	20.0
Shield	259.090	5.320	50.0	40.0	17.2	6.0
Sh.box for TCS5	264.410	0.500	50.0	40.0	-16.6 – 31.3	20.0
Shield	264.910	4.740	50.0	40.0	17.2	6.0
Sh.box for TCS6	269.650	0.500	50.0	40.0	-16.6 – 31.3	20.0
Shield	270.150	60.526	50.0	40.0	17.2	6.0
Shield	351.130	0.469	40.0	35.0	14.2	3.0
Sh.box for TCS1/2	351.775	0.500	40.0	35.0	-31.3 – 13.7	20.0
Shield	352.275	0.331	40.0	35.0	14.2	3.0
Sh.screen for MCVQ5R	358.936	0.500	50.0	40.0	13.7	2.5
Sh.screen for D3R	372.299	1.000	50.0	40.0	13.7	2.5
Shield	373.299	8.691	50.0	40.0	16.6	6.0
Sh.box for TCP1/2	381.990	0.200	50.0	40.0	-30.3 – 15.6	20.0
Shield	382.190	2.792	50.0	40.0	16.6	6.0
Passive collimator for Q6R	384.982	1.000	10.0		2.5	

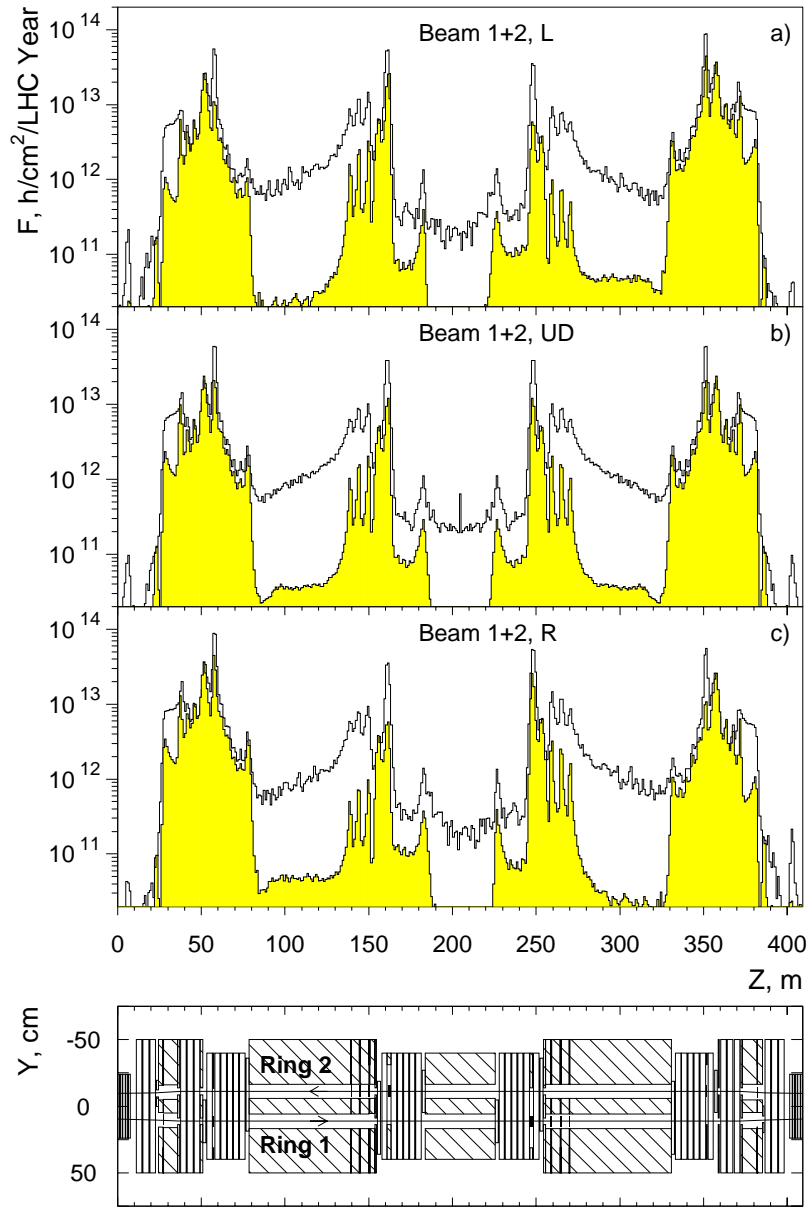


Figure 8: Fluence of hadrons around the momentum cleaning systems at a beam energy of 7 TeV: (a) generated by beams 1 and 2 in the L arc of the scoring shell, (b) generated by beams 1 and 2 in the U and D scoring arcs, (c) generated by beams 1 and 2 in the R scoring arc. The clear histogram is the case without shielding, the grey histogram is the case with full shielding. The hadron fluence is normalised to 1.0×10^{16} inelastic protons interacting inelastically in each of the two beams per year.

Table 2: The average hadron fluence, $\langle \Phi \rangle$, through the arcs of the scoring cylinder, the total leakage energy, E_s , the average hadron current, I_t , and the average energy, $\langle E \rangle$, for three cases, one without shielding and two with different shielding configurations around the collimators (per proton interacting inelastically in the scraper system).

	No shielding		Full shielding		Reduced shielding
	IR3	IR7	IR3	IR7	IR3
$\langle \Phi(L) \rangle \text{ cm}^{-2}$	1.63×10^{-4}	1.73×10^{-4}	5.87×10^{-5}	5.90×10^{-5}	6.27×10^{-5}
$\langle \Phi(UD) \rangle \text{ cm}^{-2}$	1.88×10^{-4}	2.11×10^{-4}	7.61×10^{-5}	4.94×10^{-5}	8.16×10^{-5}
$\langle \Phi(R) \rangle \text{ cm}^{-2}$	2.74×10^{-4}	2.89×10^{-4}	1.28×10^{-4}	1.19×10^{-4}	1.34×10^{-4}
$\langle \Phi \rangle \text{ cm}^{-2}$	2.00×10^{-4}	2.20×10^{-4}	8.25×10^{-5}	6.68×10^{-5}	8.78×10^{-5}
$E_s \text{ GeV}$	500	802	131	125	138
I_t	2220	2100	1139	1140	1143
$\langle E \rangle \text{ MeV}$	230	380	115	110	121

4.2 Absorbed dose to components

The annual absorbed dose in organic material around the momentum cleaning system allows one to estimate the possible impact on power cables and, with lower accuracy, on electronic elements installed in the LHC tunnel. Figure 9 shows annual absorbed dose at the position of the scoring cylinder in organic material around the momentum cleaning system for the case of inelastic interactions in the scraper systems of both beams. Peak values of the absorbed dose without shielding exceed 2×10^5 Gy per year whereas the maximum annual absorbed dose with shielding only reaches a value of 3.5×10^4 Gy. As in the case of the hadron fluence, the main peaks are concentrated around the TCS1-TCS3 secondary collimators and the shielding screens. Even with the shielding, annual absorbed doses exceed significantly the suggested tolerances of electronic elements (100 Gy – 1000 Gy [15]).

Whereas in the case of the hadron fluence the efficiency of the shielding varies from a factor 2 or 3 up to a factor 100 with an average value of about 2.4, the shielding factor for absorbed dose can reach values of up to 1000, with an average value of around 8.1. The average shielding efficiency for hadron fluence and absorbed dose in the scoring shell is summarised in Table 3. Again it can be noted that the full shielding is most efficient in regions where the absorbed dose is not the most important, *i.e.* between the quadrupoles Q4 and Q5.

4.3 Reduced shielding

Since the long drift sections between the Q4 quadrupoles and between the Q5 quadrupole and the TCS6 collimator do not contribute much to either the total hadron fluence or the total absorbed dose (this with or without shielding, see from Figs 8 and 9), it should be possible to leave these sections without shielding. However it is still necessary to shield the small region between the Q5 quadrupole and the TCS6 collimator because of

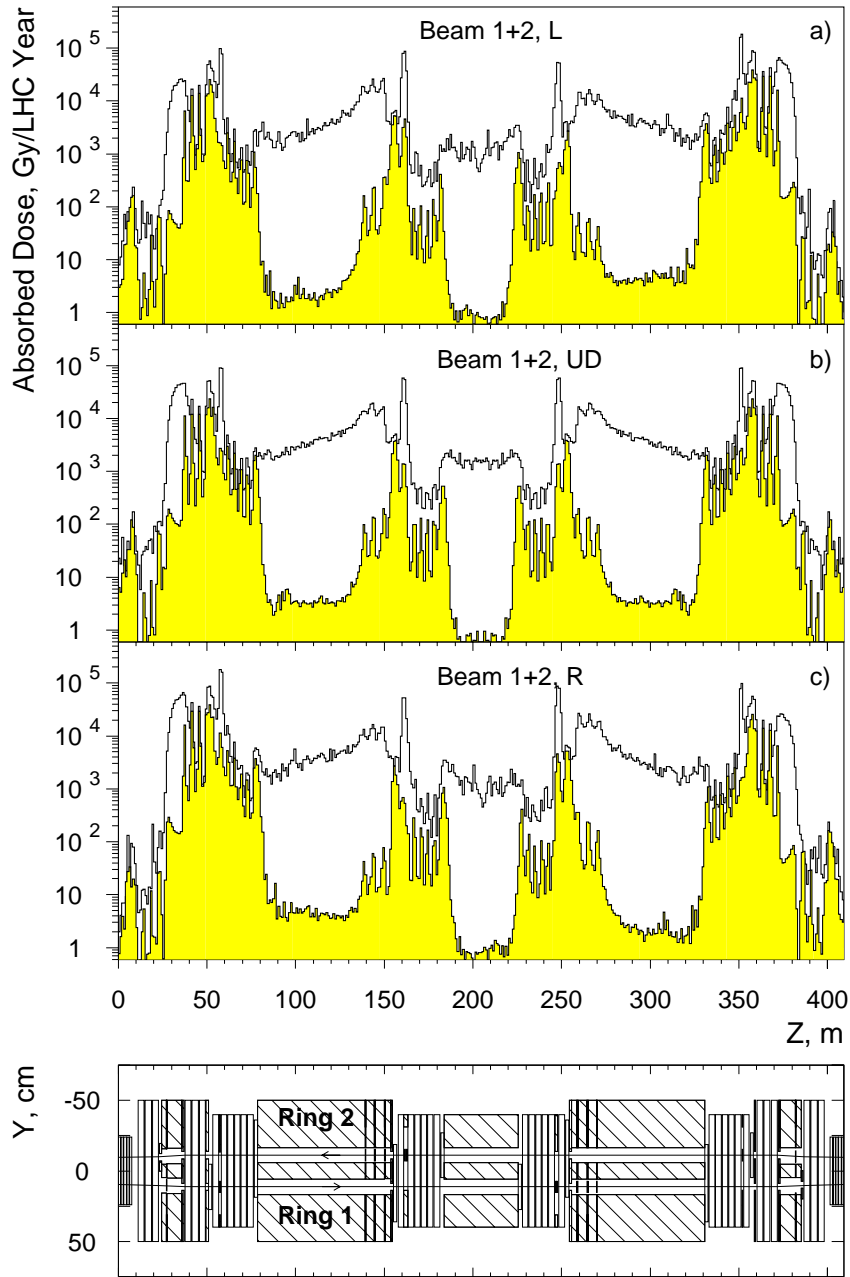


Figure 9: Annual absorbed dose in organic material around the momentum cleaning system for losses in both of the two rings: (a) generated by beams 1 and 2 in the L arc of the scoring shell, (b) generated by beams 1 and 2 in the U and D scoring arcs, (c) generated by beams 1 and 2 in the R scoring arc. The clear histogram is the case without shielding, the grey histogram is the case with full shielding. The absorbed dose is normalised to 1.0×10^{16} inelastic protons interacting inelastically in each of the two beams per year.

Table 3: Average efficiency of full shielding for hadron fluence and absorbed dose

Shielding	Hadron fluence				Absorbed dose			
	L	UD	R	<>	L	UD	R	<>
Full	2.8	2.5	2.2	2.4	7.5	8.9	7.0	8.1
Reduced	2.6	2.3	2.0	2.3	5.3	5.5	5.1	5.3

the three secondary collimators. A possible reduced shielding configuration is illustrated in Figure 10. A new series of simulations was performed with this reduced shielding configuration. The resulting longitudinal distributions of hadron fluence and absorbed dose around momentum cleaning in the scoring shell are presented in Figures 11 and 12. As with the full shielding, localised sources give the main contribution to fluence and dose. They determine the average characteristics of the hadron leakage (see the last column in Table 2) and the maximum radiation doses to electronic components and cable insulation. The last row in Table 3 shows that the average efficiency for hadron fluence reduction of the reduced shielding is 90 – 95 % of that for the full shielding. In the case of the absorbed dose, the shielding efficiency is 62 – 70% of the full shielding configuration. The reduced shielding variant requires about 560 tons of iron and 96 tons of concrete, 2.5 times smaller than that required for the full shielding configuration.

4.4 Induced radioactivity of shield and magnets

Remanent dose rates from activated shielding and magnets will determine the access time of personnel to these areas after beam operation. The contact dose rates on the surface of the iron shield and magnets in the momentum cleaning section was obtained using the so-called ω - factor which has an approximate value of 10^{-8} Sv/h per star/cm³ produced per second [16] for the case of 30 days of irradiation and 1 day of cooling. Contact dose rates as a function of longitudinal position for both rings are presented in Figure 13. Dose rates are normalised to 1.0×10^9 protons per second interacting in the momentum cleaning system for each ring. It will be seen from this figure that the contact dose rate reaches a maximum values of 3 mSv/h near the first secondary collimators TCS1 of each beam and near the bare coil ends of of the dipole and orbit corrector magnets. The intensity of these peaks are mostly associated to local proton losses of the beam impacting directly on these elements. The dose rate in these limited areas exceeds significantly the value of 100 μ Sv per hour. It should be noted that without shielding the dose rates from induced radioactivity in the collimator jaws, the front bare coils and the beam pipes will exceed values of 100 mSv h⁻¹.

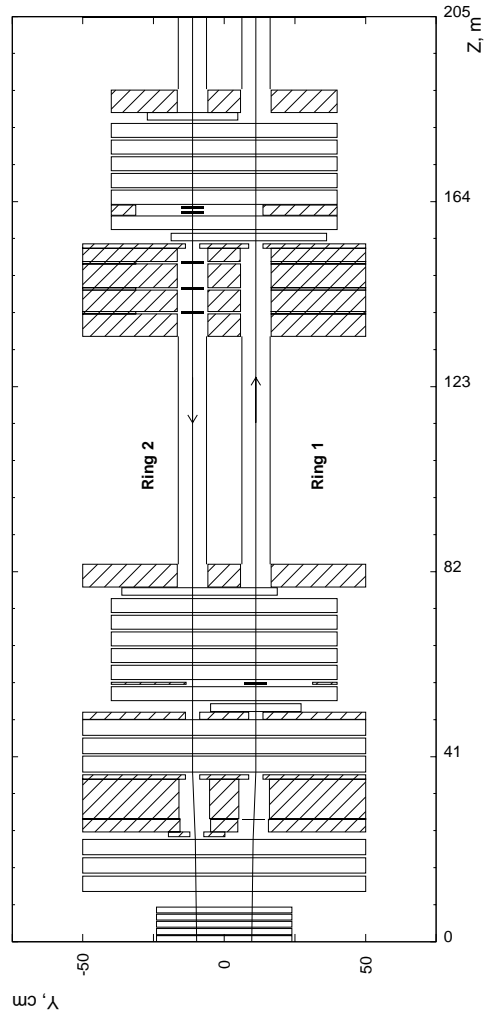


Figure 10: Longitudinal section through one half of the cleaning section for the reduced shielding configuration.

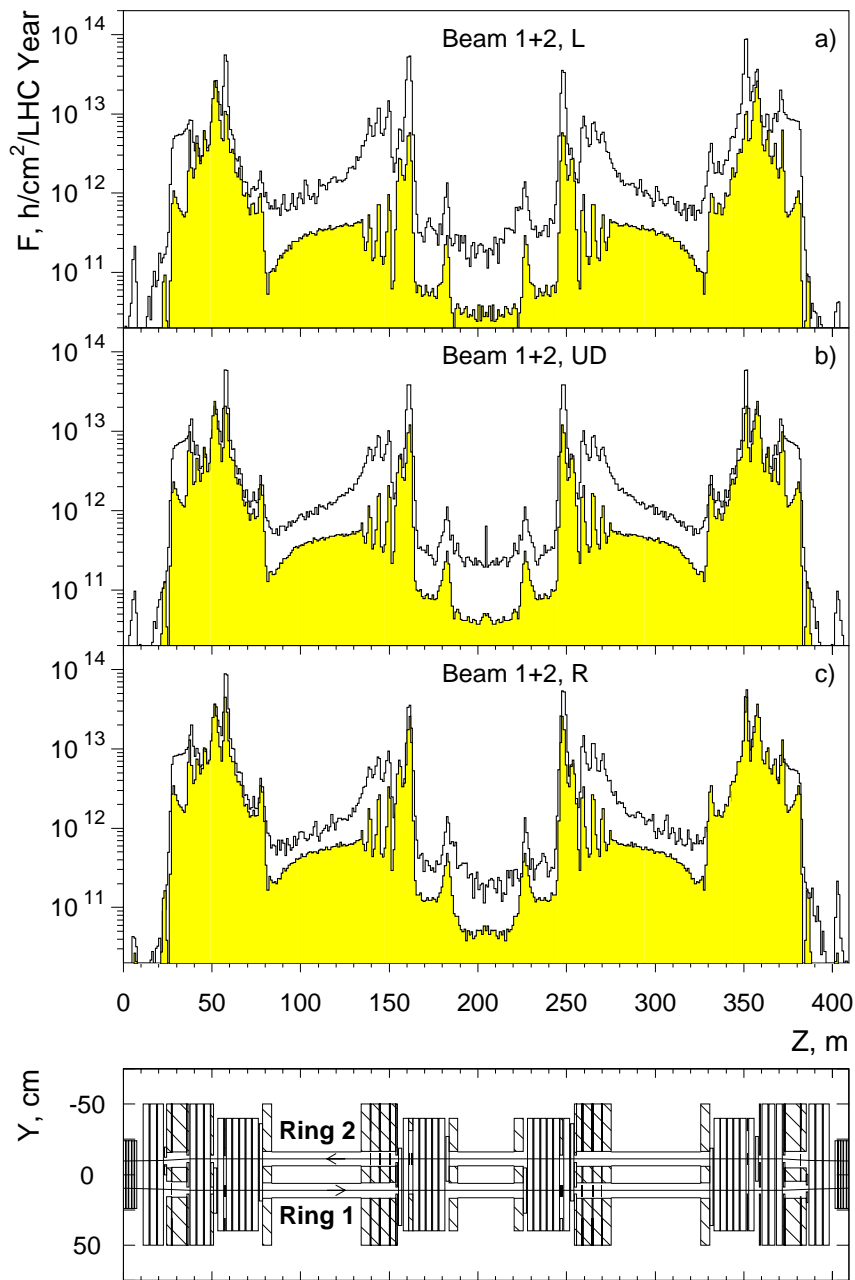


Figure 11: Fluence of hadrons around the momentum cleaning systems at a beam energy of 7 TeV: (a) generated by beams 1 and 2 in the L arc of the scoring shell, (b) generated by beams 1 and 2 in the U and D scoring arcs, (c) generated by beams 1 and 2 in the R scoring arc. The clear histogram is the case without shielding, the grey histogram is the case with the reduced shielding. The hadron fluence is normalised to 1.0×10^{16} inelastic protons interacting inelastically in each of the two beams per year.

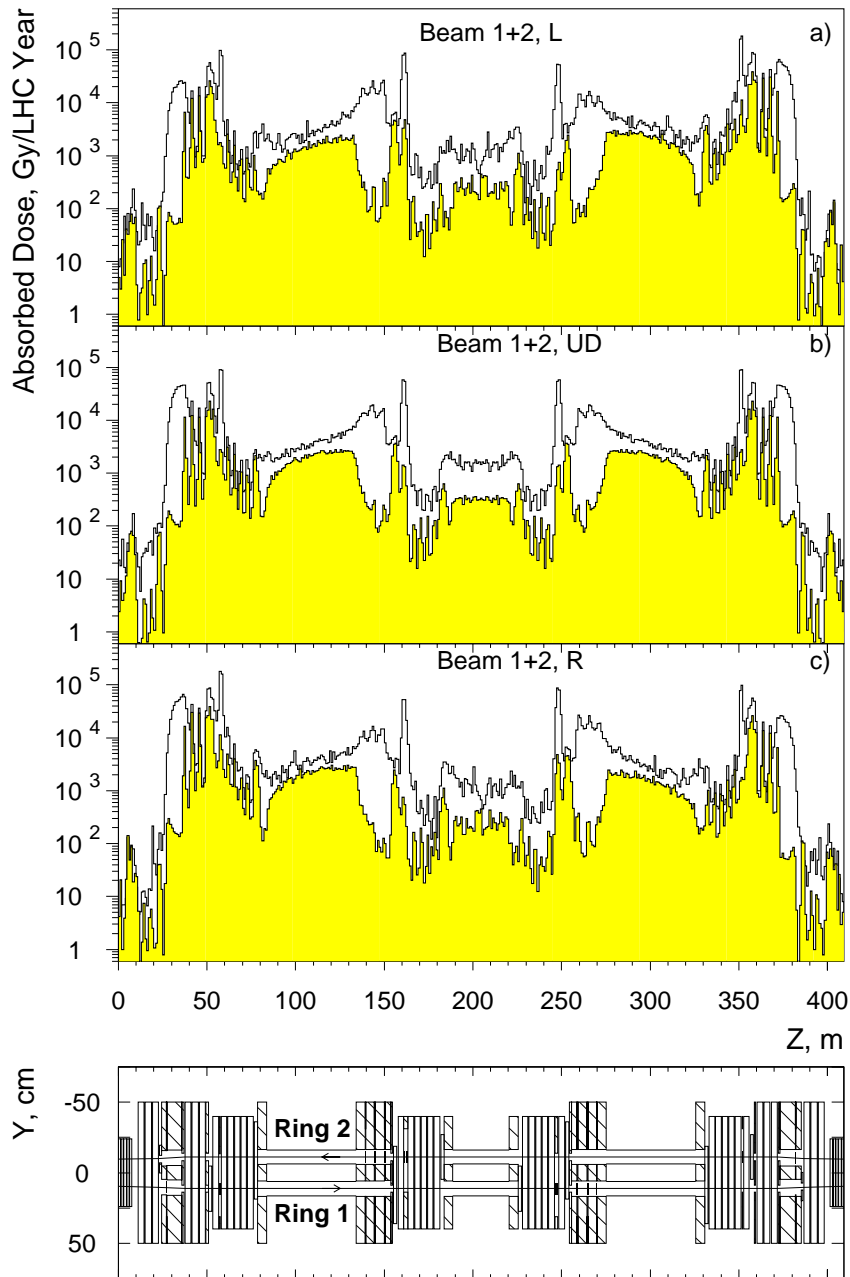


Figure 12: Annual absorbed dose in organic material around the momentum cleaning system for losses in both of the two rings: (a) generated by beams 1 and 2 in the L arc of the scoring shell, (b) generated by beams 1 and 2 in the U and D scoring arcs, (c) generated by beams 1 and 2 in the R scoring arc. The clear histogram is the case without shielding, the grey histogram is the case with the reduced shielding. The absorbed dose is normalised to 1.0×10^{16} inelastic protons interacting inelastically in each of the two beams per year.

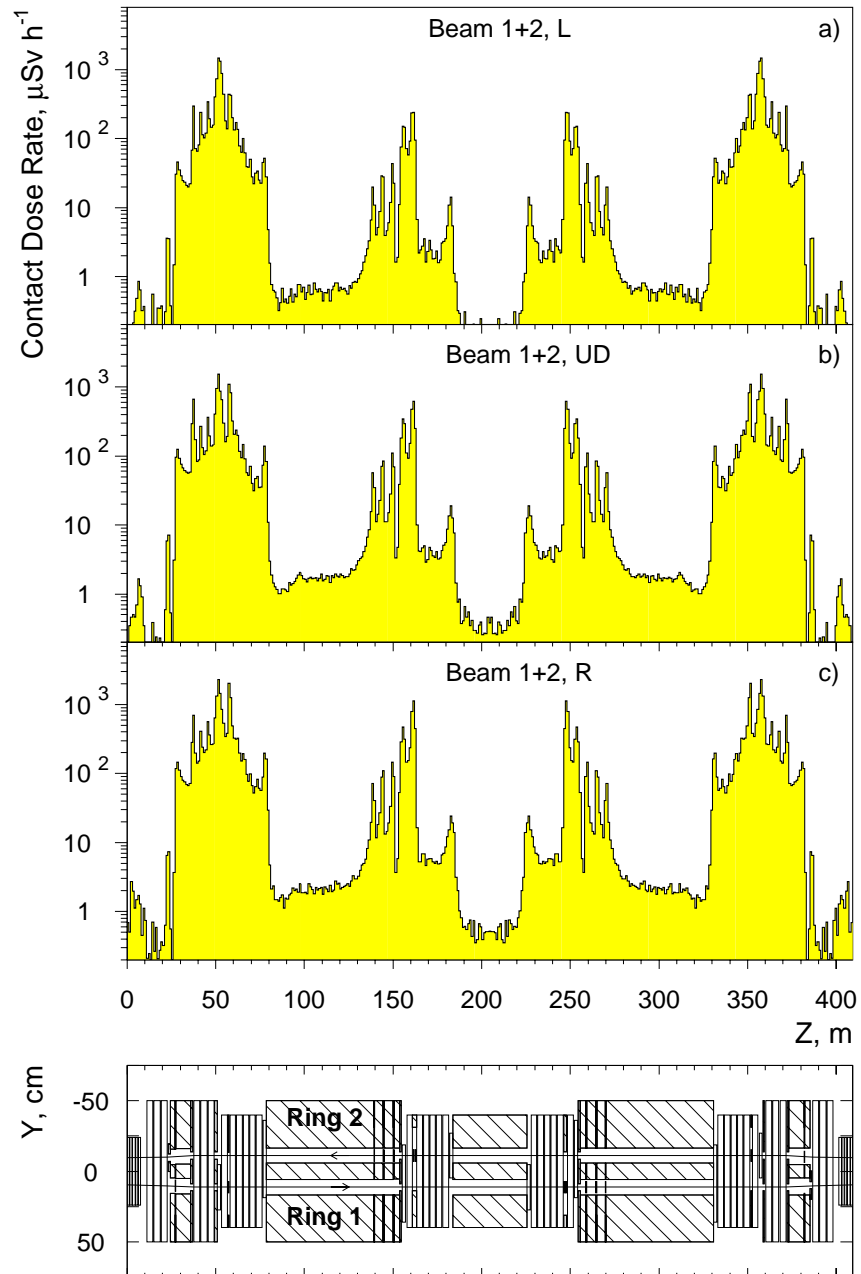


Figure 13: Contact dose rates on the surface of the iron shield and magnets in the momentum cleaning section: (a) left surface L; (b) up-down surface UD; (c) right surface R. The contact dose rate is normalised to an inelastic interaction rate of 1.0×10^9 protons per second in each of the two rings.

5 Conclusions

- In its full configuration, the shielding reduces the average hadron fluence by a factor of 2.4 and the average absorbed dose by a factor 8.1.
- In its reduced configuration, the shielding reduces the average hadron fluence by a factor of 2.3 and the average absorbed dose by a factor 5.3.
- Peaks of absorbed dose reach values of 3.5×10^4 Gy/year even with shielding.
- The contact dose rate reaches maximum values of 3 mSv per hour, and there are limited areas where dose rates exceed significantly value of $100 \mu\text{Sv}$ per hour.
- The low efficiency of the shielding is determined by the inability to place sufficient shielding around the scrapers/collimators themselves.
- The full shielding design requires about 1400 tons of iron sitting on 240 tons of concrete.
- The reduced shielding design requires a shield whose weight is 2.5 times smaller (560 tons of iron and 96 tons of concrete) than with the full shield configuration, without seriously jeopardising shielding efficiency.

References

- [1] G. R. Stevenson, *Shielding high-energy accelerators*, Proc. of the Tenth Course of the International School of Radiation Damage and Protection, *Accelerator Radiation Protection*, Erice, Sicily, October 2–9 2001, Rad. Prot. Dosim. 96 (2001) 359.
- [2] Optics of a two-stage collimation system, J.B. Jeanneret, Phys. Rev. ST Accel. and Beams, 1, 081001, December 1998.
- [3] Optics solutions for the collimation insertions of LHC, D.I. Kaltchev et al., *Proceedings of the PAC99 Conference, New-York, 1999*, edited by A. Luccio and W. MacKay, p. 2623 and CERN LHC Project Report 305, 1999.
- [4] I. L. Azhgirey, I. S. Baishev, J. B. Jeanneret, I. A. Kourotchikine and G. R. Stevenson, *Cascade simulation studies for the momentum cleaning insertion of LHC*, LHC Project Note 263, (2001).
- [5] M. Höfert, K. Potter and G. R. Stevenson, *Summary of Design Values, Dose Limits, Interaction Rates etc. for use in estimating Radiological Quantities associated with LHC Operation*, CERN Internal Report CERN/TIS-RP/IR/95-19.1 (1995).
- [6] *INB Rapport préliminaire de Sûreté du LHC* (1999).
- [7] J. B. Jeanneret, D. Leroy, L. R. Oberli and T. Trenkler, *Quench levels and transient beam losses in LHC magnets*, LHC Project Report 44, (1996).

- [8] I. L. Azhgirey, I. S. Baishev, J. B. Jeanneret and I. A. Kourotchkin, *Power deposition in superconducting magnets in the momentum cleaning insertion*, LHC Project Note 286, (2002).
- [9] I. L. Azhgirey, I. A. Kurochkin and V. V. Talanov, *MARS program complex development for radiation aspects of electro-nuclear devices design*, in: *Materials of XV Workshop on Charged Particle Accelerators*, Vol. 2, p. 270, Protvino, in Russian (1996).
- [10] T. Trenkler and J-B. Jeanneret, *K2: A software package evaluating collimation systems in circular colliders (Manual)*, CERN Internal Report SL/Note 94-105 (AP) (1994).
- [11] I. Azhgirey, I. Baishev, N. Catalan-Lasheras and J. B. Jeanneret, *Cascade simulations for the betatron cleaning insertion*, CERN LHC Project Note 121 (1997); CERN LHC Project Report 184 (1998).
- [12] I. L. Azhgirey, I. Baishev, I Dawson, J. B. Jeanneret, G. R. Stevenson and H. H. Vincke, *Radiation studies of the LHC betatron scraping region at point 7*, CERN Internal Report CERN/TIS-RP/IR/99-01 (1999).
- [13] J. B. Jeanneret, *A specification for the momentum cleaning*, LHC Project Note 115 (1997).
- [14] G. R. Stevenson, A. Fassò and J. M. Zazula, *Estimation of parameters of radiological interest for the scraper system of the LHC*, CERN Internal Report CERN/TIS-RP/IR/92-25 (1992).
- [15] R. Rausch, *Electronics for the LHC tunnel, Radiation Test Results*, TCC Seminar, May 18 (2001).
- [16] R. H. Thomas and G. R. Stevenson, *Radiological safety aspects of the operation of proton accelerators*, Technical Report Series No.283, IAEA Vienna (1988).